

# The Effect of GBFS as reinforced fill on Reinforced Wall with Bamboo Cellular Reinforcement

**Kamlesh Vasant Madurwar<sup>1\*</sup>, Avinash N. Shrikhande<sup>2</sup>**

<sup>1</sup> *Research Scholar, Kavikulguru Institute of Technology and Science, Ramtek, Nagpur.*

<sup>2</sup> *Professor, Kavikulguru Institute of Technology and Science, Ramtek, Nagpur.*

## **Abstract**

The steel manufacturing industries in India produces huge amounts of granulated blast furnace slag (GBFS) which demands large dumping area. The dumping of GBFS affects the surrounding ecosystem. In the current experimental work, an attempt has been made to utilize GBFS as a substitute fill in the reinforced wall structure. For carrying out the experimentation a tank with dimensions 750 mm × 400 mm × 600 mm was fabricated using mild steel plates. A mattress of cellular reinforcement was prepared with the help of bamboo. *Dandrocalthus strictus* was the specie of bamboo utilized for making the cellular reinforcement. The geocells were prepared with two different diameters i.e., 50 mm and 60 mm and two different heights 10 mm and 20 mm. These constitute four different mattresses viz. 50 – 10, 50 – 20, 60 – 10, and 60 – 20. Five different Models were tested. Model 1 was unreinforced fill, and the rest of the models contained each variety of cellular reinforcement mattress. The experimental setup was tested under strip loading condition. The results show that reinforced wall with 60 – 20 bamboo cellular reinforcement had the greatest performance when compared with the other models.

**Key Words:** GBFS, Geocell, reinforced fill, cellular reinforcement, mattress

## **1. Introduction**

Road networks are the backbone of a country's development. There are many components which are constructed during the development and expansion of road network. Reinforced wall is one of those essential components which has gained popularity in the recent development due to its simplicity in construction, low costs and deformation capacity without undergoing damage [1]. The approach of a flyover is constructed with a reinforced wall. The reinforced wall is nothing but a mechanically stabilized earth retaining wall. Its components include retaining wall, backfill/reinforced fill material and reinforcement [2]. The tensile strength of the reinforcement integrated with shearing strength of soil results into a composite action which

is responsible for resisting the load and deformations [3]. Generally, a granular material is used as a reinforced fill material and polymer/steel is used as material of reinforcement. When polymer is used as reinforcement it is either converted into a cloth which is known as geosynthetics or it is constituted into a grid framework and is known as geogrids. Geosynthetic and geogrids are modern, light weight but very costly materials. In the early developments stages of reinforced wall generally steel straps and mat were used [4]–[6]. But the utilization of sand, steel/polymer tends to deplete the natural resources and causes carbon emissions which in turn disturbs the ecological balance of the environment.

Stepping towards sustainability, the global researchers had started replacing sand with a judicious substitute. The substitutes are sourced from the industrial wastes. Lal et.al. had used fly ash as a reinforced fill in the mechanically stabilized earth retaining structure [7]. Pant et.al. deployed bottom ash as a reinforced fill material [8]. Table 1 lists some of the materials which are used as reinforced fill materials. Any material cannot be used directly as a reinforced fill but after satisfying gradation strength and electrochemical properties can be used as reinforced fill [8]. Whenever such industrial are used as reinforced fill they not only bring economy and sustainability in construction but also mitigate the environmental concerns related to the disposal of such waste.

**Table 1:** Material that are used as reinforced fill in the MSE retaining wall

Sr. No.	Material	Source
1	Fly ash	[7]
2	Bottom ash	[8]
3	Pond ash	[9]
4	Copper slag	[10]
5	Imperial melting furnace slag	[11]
6	Waste foundry sand	[12]
7	Shredded rubber waste	[13]
8	Construction and demolition waste	[14]
9	Granulated blast furnace slag	[15]

Out of all these wastes granulated blast furnace slag (GBFS) is a waste which is produced in huge quantities globally. China is the global leader in production of GBFS and India follows China. GBFS is a waste which evolves from the iron ore processing industry. In the iron ore processing furnace, the raw ore of iron along with a lime source and coke is added. The lime source such as dolomite acts as a flux agent. During the processing of ore at 1400 – 1600°C iron being of higher specific gravity settles at bottom and the molten slag floats at the top. This molten slag is then removed and cooled rapidly with water jets. The rapid cooling results into an amorphous slag granules which is known as granulated blast furnace slag [16], [17].

As reinforcements steel and polymers have been predominantly used. But they are costly and their development is associated with pollution. These materials can be very well replaced by some natural fibrous material which possess properties similar to those of steel and polymer. So, bamboo is one such material which possess tensile strength which is adequate for utilization as reinforcement in MSE retaining wall [18]. Since bamboo is a natural material, it has a tendency to degrade with time. For increasing the life of bamboo some treatment methods are available which increase its durability. Ju et.al used electrochemical silver modification of hemicellulose and lignin for increasing the durability of bamboo [19].

Therefore, the current experimental work uses GBFS as a reinforced fill material and bamboo as a reinforcing material. Utilization of these materials not only achieves economy but also increases the sustainability. Bamboo strips were drawn and moulded into geocells. The geocells were connected to each other with a polymer to form a reinforcement mattress. The effect of the geocell mattress and GBFS as a reinforced fill was studied in an experimental set simulating MSE retaining wall.

## **2. Materials and methods**

### **2.1 Materials**

In the present study two materials were used. The first one was granulated blast furnace slag (GBFS) which is a byproduct of steel industry and the other was seasoned bamboo. The GBFS was procured from the iron and steel industry situated at Bhilai, Chhattisgarh. At Bhilai steel plant, the GBFS was water quenched. The specie of bamboo utilized in the present work was ‘Dendrocalamus Strictus’ and was procured from Maharashtra Bamboo Development Board, adjacent to Katol Naka, Nagpur, Maharashtra, India.

### **2.2 Material characterization**

Before utilizing GBFS it was very important to study the physical, chemical, and morphological properties. Therefore, GBFS was tested under X-Ray Fluorescence (XRF) for chemical composition, X-Ray Diffraction (XRD) for phase identification, Scanning Electron Microscopy (SEM) for morphological studies and Particle Size Distribution for observing the distribution different size fraction of particles. Apart from these properties some engineering properties of GBFS were also found.

#### **2.2.1 X-Ray Fluorescence (XRF) test**

X-Ray Fluorescence test was performed by using X-Ray Fluorescence Spectrometer. The facility was available in a Laboratory at Department of Physics, Rashtrasant Tukadoji Maharaj Nagpur University (R.T.M.N.U), Nagpur to ascertain the percentage of chemical oxide present

in the GBFS. The results of the experiments for the chemical composition are shown in Table 1. This is very important as it can help in tracing out the hazardous material inside GBFS. The major oxides that were present inside GBFS were calcium oxide (CaO), silicon dioxide (SiO<sub>2</sub>) and aluminum oxide (Al<sub>2</sub>O<sub>3</sub>). These three oxides constitute 87.36 % of the total volume of GBFS. Magnesium oxide was also present in substantial quantities (7.61%). The other oxides which were present in minor quantities were titanium oxide, chromium oxide, manganese oxide, phosphorous pentoxide, strontium oxide, zirconium oxide, and barium oxide.

**Table 1:** Chemical composition of GBFS

Oxides	CaO	SiO <sub>2</sub>	Al <sub>2</sub> O <sub>3</sub>	MgO	SO <sub>3</sub>	K <sub>2</sub> O	Fe <sub>2</sub> O <sub>3</sub>	Na <sub>2</sub> O	Others
%	43.36	31.76	12.24	7.61	1.75	0.6	0.46	0.38	1.84

### 2.2.2 X-Ray Diffraction (XRD) test

The X-Ray Diffraction test was conducted using the X-Ray Diffractometer available with Rashtriya Uchcharat Siksha Abhiyan (RUSA) cell, R.T.M.N.U., Nagpur. The scanning was conducted with  $2\theta$  ranging from  $10^\circ - 70^\circ$  with a step size of 0.04 and at a scanning rate of  $5^\circ$  per minute. The test helps in identifying whether the material is crystalline, amorphous, or semicrystalline. The  $2\theta$  versus intensity plot of GBFS shows a broad diffused hump ranging from  $20^\circ$  to  $40^\circ$  as shown in Figure 1. This hump is indicative of the amorphous nature of GBFS. The graph presents some peaks between  $20^\circ$  to  $30^\circ$ , which shows the presence of crystalline quartz (Q) at  $2\theta$  equal to  $20.88^\circ$  and  $26.6^\circ$ .

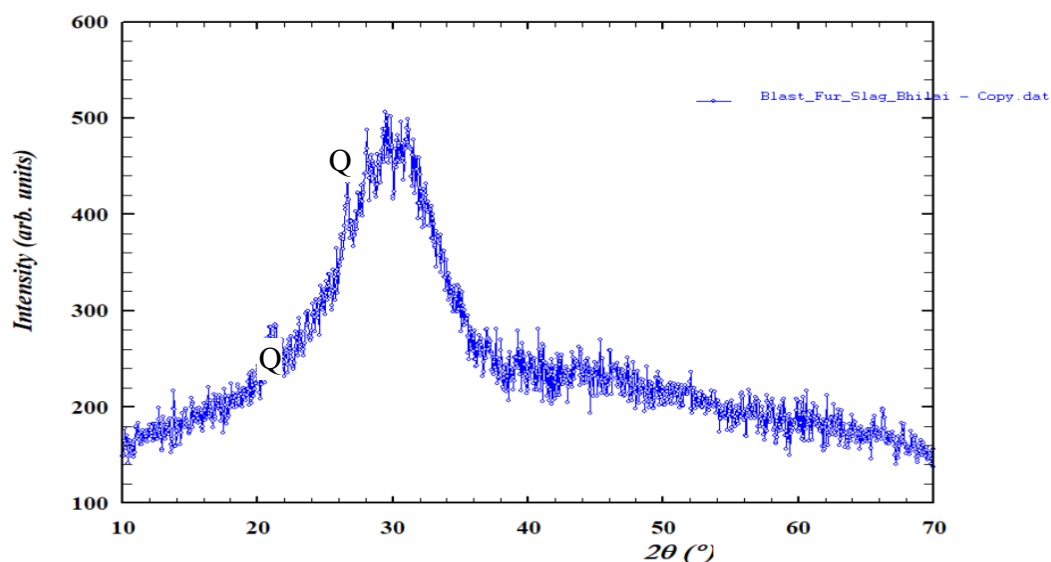


**Figure 1:** X-Ray diffractogram of GBFS

### 2.2.3 Scanning Electron Microscopy (SEM)

Scanning electron microscopy used to carry out the morphological studies was available in a Laboratory at Department of Physics, R.T.M.N.U, Nagpur. Morphological study helps in

determining the different shapes, size, and porosities inside the particles. Figure 2 shows the backscattered image of GBFS particles which was captured at a voltage of 5kV. The scale for the captured image was 1 $\mu$ m. The microparticles had irregular shapes and were solid in nature. Some of the particles in GBFS had size even less than 1 $\mu$ m.

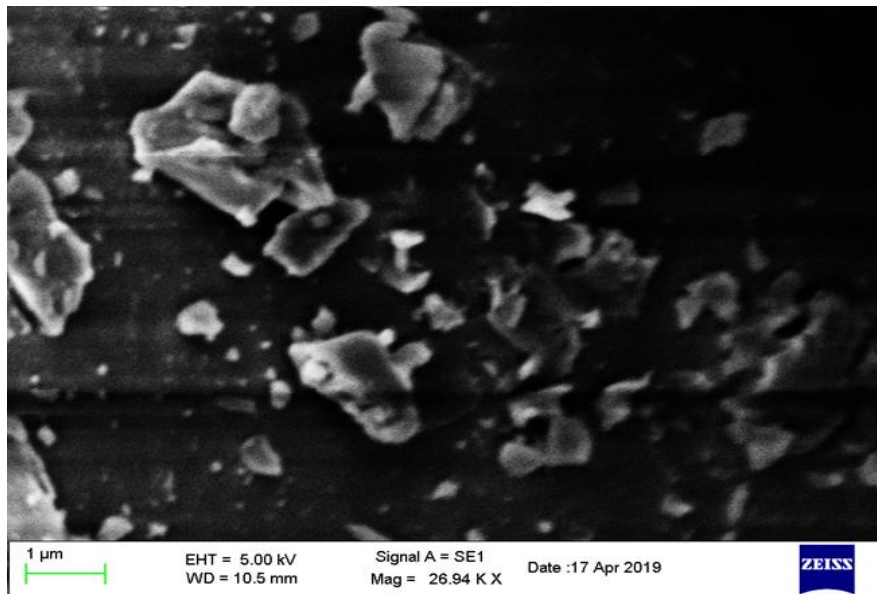


**Figure 2: Scanning electron microscopy image of GBFS particles.**

#### 2.2.4 Particle Size Distribution (PSD)

The particle size distribution curve as manifested in Figure 3 was plotted with the help of results obtained from sieve analysis. Since GBFS resembles sand, the procedure applied for particle size distribution of sand was also followed for GBFS.

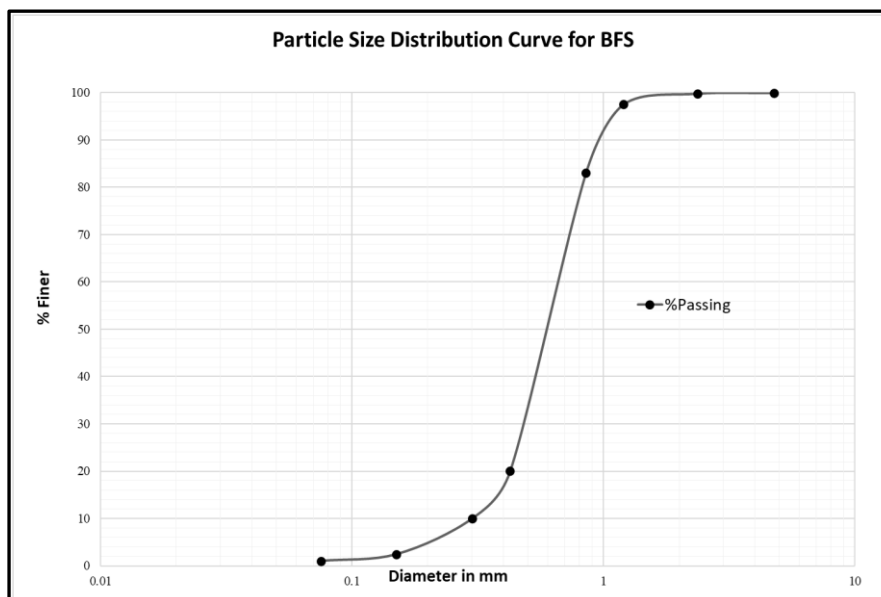


**Figure 3: Particle size distribution curve of GBFS**

The set of sieves that were used for the analysis were 4.75 mm, 2.36 mm, 1.18 mm, 850-micron, 425-micron, 300-micron, 150-micron and 75-microns. These set of sieves were attached with a pan at bottom and the top sieve was fitted with a lid after pouring GBFS into the top sieve. 1 kg of GBFS was used for the test. These assembly of sieve set was mounted on a sieve shake which induced standard vibrations for shaking. The shaking continued for 5 minutes. The weight retained on each sieve and pan was noted and percentage finer was calculated. The curve for particle size distribution was plotted between aperture size of sieve in mm and % finer on a semi-log scale on x-axis.

### 2.2.5 Engineering Properties of GBFS

The engineering properties which were found for GBFS are displayed in Table 2. These soil engineering properties will help us in assessing the behaviour of GBFS as soil.

**Table 2:** Soil engineering properties of GBFS

Properties	Unit	Value	Properties	Unit	Value
Specific Gravity	-	2.07	Uniformity Coefficient ( $C_u$ )		2.16
Plasticity		Non-Plastic	Coefficient of Curvature ( $C_c$ )		1.18
Mean Particle Size ( $D_{50}$ )	mm	0.6	Cohesion	kN/m <sup>2</sup>	8.5
D <sub>10</sub>	mm	0.3	Angle of internal friction		41°
D <sub>30</sub>	mm	0.48	$e_{max} / e_{min}$	gm/cm <sup>3</sup>	1.268/1.156
D <sub>60</sub>	mm	0.65	Permeability	Highly Permeable	

### 2.3 Bamboo – A Cellular Reinforcement

It is already well known that bamboo is a flexible material. Therefore, the bamboo was utilized for making the mattress. *Dandrocalamus Strictus* is a bamboo specie which was used in formation of cellular reinforcement. For the formation of cellular reinforcement 1 mm thick strips were cut from the circumferential thickness of bamboo. These strips were drawn in two widths, 1) 10 mm and 2) 20 mm. The decided cellular reinforcement diameter was 50 mm and 60 mm. The length of strip required was an addition of circumferential length of cellular reinforcement and lap length. The lap length was taken as 150 mm. Therefore, the total length required for 50 mm diameter cell was 190 mm and for 60 mm was 210 mm. An epoxy adhesive was used to join the lap length of bamboo strips. So, considering the two diameters (50 mm and 60 mm) and two width (10 mm and 20 mm) of strips, has resulted in four different dimensions of cellular reinforcement. A mattress of cellular reinforcement with homogeneous

dimensions was formed. The cellular reinforcements were attached to each other with the help of a polymer tag.

## 2.4 Model Testing

### 2.4.1 Experimental Setup

Model tests were conducted to study the behaviour of the retaining walls without and with reinforced fill. To carry out the tests, a custom designed experimental test set up was fabricated. The dimensions of test tank were 750 mm long  $\times$  400 mm wide  $\times$  600 mm high. The test tank was fabricated using 20 mm thick mild steel sheet and angles to ensure minimum deformations. One side of test tank was fitted with Perspex sheet to observe the failure pattern of backfill. The model test wall was at 150 mm behind the front face of the tank to accommodate the wall deformations, including the failure deformations during the collapse stage. The scope of testing program includes study of cellular reinforced soil retaining wall with full height of facing. A stiff plywood of 10 mm thickness, with 600 mm height and 380 mm in width was used to stimulate the independent full height of facing. The total experimental setup along with retaining wall is shown in Figure 5.

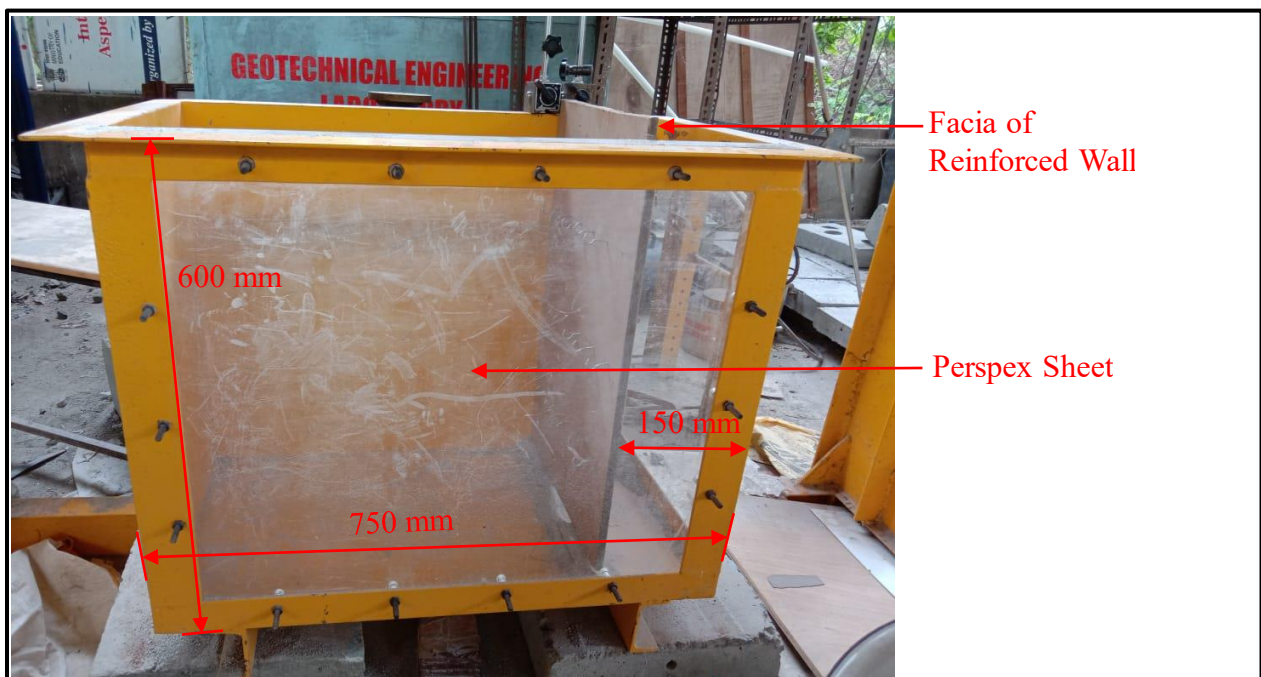


**Figure 5:** Experimental test setup

### 2.4.2 Arrangement of Test Setup

The faces of the tank fitted with a retaining wall and was hinged at the base of the tank and the verticality was maintained with the help of clamps. The tank was filled with GBFS in two ways a) without cellular reinforcement mattress and b) with cellular reinforcement mattress. The

total height of fill in the tank was 600 mm. When reinforcement mattresses were added to the fill, they were laid in three layers at a separating distance of 150 mm. The length of each mattress was  $0.7H$  (where  $H$ , is height of the facing element). Stainless steel hooks were installed in the retaining wall for attaching the mattress. For setting up the test model with reinforcement mattress, 150 mm thick GBFS layer was laid inside the tank. Over this layer first reinforcement mattress was laid. This procedure was repeated thrice inside the tank and a fourth and final layer of GBFS with 150 mm thickness was used to complete the test setup. Every layer of reinforcement was marked as an edge with the help of coloured sand. The test setup with backfill, reinforcement mattress and load application can be seen from Figure 6. This was to observe the failure surface through Perspex sheet placed on one side of the test tank. The GBFS was filled with rainfall technique to achieve around 85 % of relative density. The iterations used in the present experimental work are detailed in Table 3.

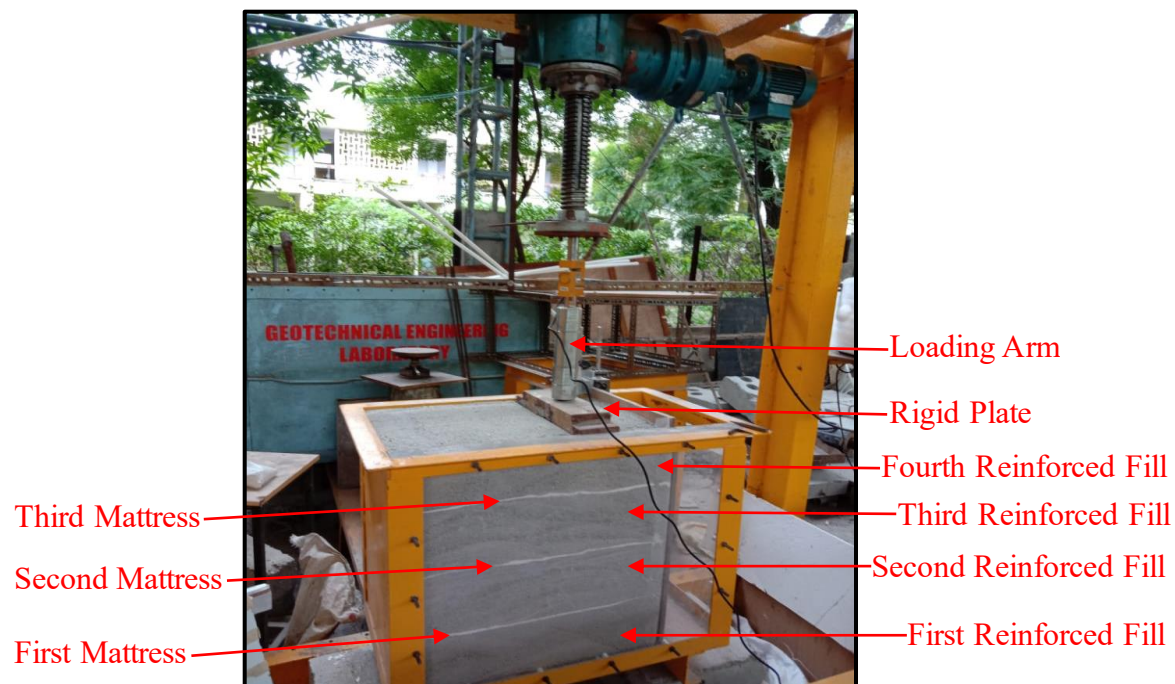


**Figure 6:** Backfilled reinforced wall

### 2.4.3 Instrumentation and Data Acquisition

A load cell having capacity of 25 kN was used for measuring vertical load. Two numbers of non-spring type LVDTs, each having total displacement capacity of 50 mm, were used for measuring the horizontal deformation. Load was recorded to an accuracy of 0.1 N and the deformations were measured with 0.01 mm accuracy. The load was applied through a load cell which was placed centrally on a rigid plate of 10 mm thickness. All the LVDTs along with the load cell were calibrated before use and are connected to data logger system as shown in Figure



7. All these tests were carried out at Geotechnical Engineering Laboratory, Civil Engineering Department, Visvesvaraya National Institute of Technology (VNIT), Nagpur.

**Table 3: Iterations of experiment**

Type	Cellular Reinforcement Mattress Diameter & Height	Spacing Reinforcement (mm)	Reinforcement Length (mm)
Model 1	--	--	--
Model 2	50 mm & 10 mm	150	0.7H
Model 3	50 mm & 20 mm		
Model 4	60 mm & 10 mm		
Model 5	60 mm & 20 mm		



**Figure 7:** Experimental set up reinforced wall with DAQ system

### 3. Results and Discussion

The data for all the model testing was assessed from the data acquisition system fitted with the experimental setup. The interpretation and discussion on results are scripted in the forthcoming section.

### 3.1 Model Testing

In case of unreinforced backfill wall (Model 1) test, as the clamps attached for maintaining the verticality of wall was removed, the wall collapsed instantaneously. Any kind of load was not applied. The most probable reason for failure is that the wall was hinged at the base of the tank. A uniformly varying load having intensity of zero at top and  $K_a\gamma H$  (where  $H$  is the filling height) at the base was applied due to the backfill material on the wall. As it is already known that hinge allows rotation, the wall rotated due to load and never resisted the load. This type of failure was not observed in case of reinforced wall. The reinforcement mattress provided within the reinforced fill inside the tank not only maintained the verticality of wall but also increased the load carrying capacity due to surcharge loading.

Figure 8, Figure 9, Figure 10, and Figure 11 are the load vs deformation response of various models with reinforced fill. These plots show the response for horizontal deflection of wall as well as vertical settlement of reinforced fill due to surcharge loading. Figure 12 shows the cumulative response of all the models, where it could be noticed that increase in load also increases the deformation in vertical and horizontal direction. The load vs deformation curve of vertical settlement and horizontal deflection look alike. In the Model 2 the utilization of 50 – 10 mattress have sustained a maximum load of 1.69 kN at which the lateral wall deflection was 30.47 mm and vertical settlement was 31.47 mm. In the horizontal deflection curve, after a deflection of 19.61 mm the load suddenly dropped till 1.03 kN after which it again started increasing. Such phenomenon was also observed in case of vertical settlement.

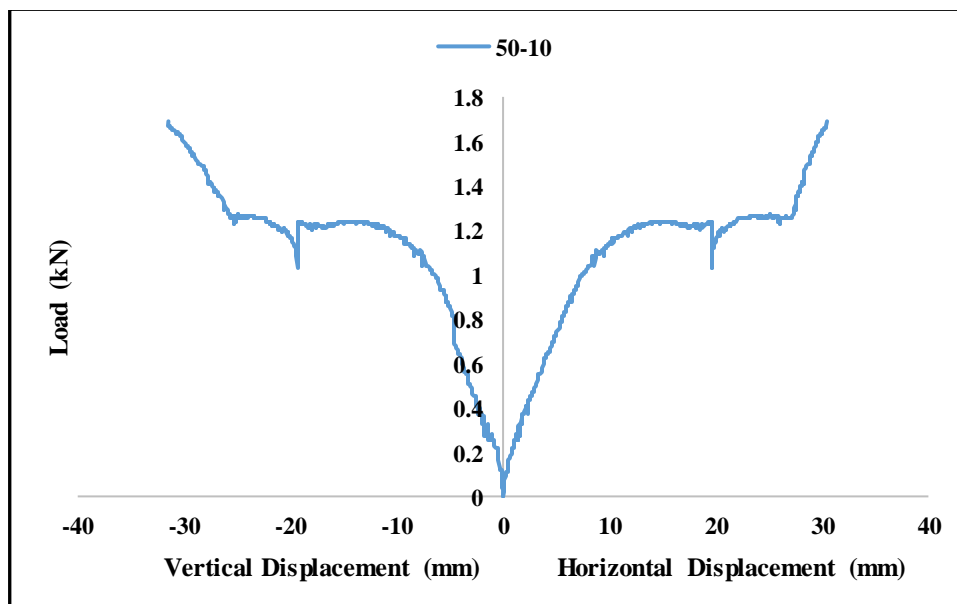


**Figure 8:** Load vs displacement curves for 50 – 10 reinforcement mattress.

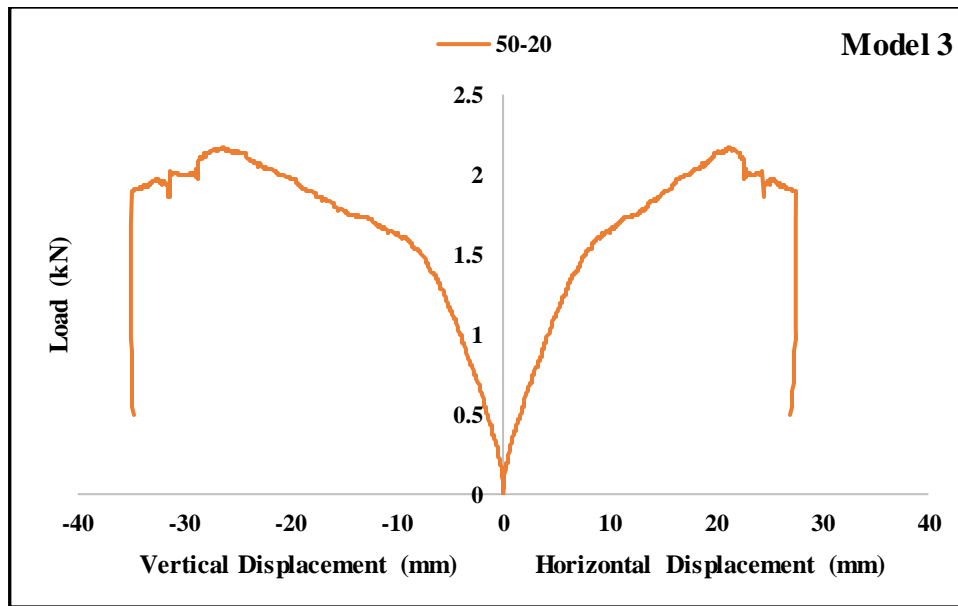


**Figure 9:** Load vs displacement curves for 50 – 20 reinforcement mattress.

In the Model 3 the usage of 50 – 20 reinforcement mattress have elevated the load carrying capacity to 2.17 kN. At this load, the horizontal deflection of wall and vertical settlement of reinforced fill was observed as 21.28 mm and 26.43 mm respectively. A 10 mm increase in height of strip has resulted in an increase in load carrying capacity by 0.48 kN which accounts for 28.4% increase when compared with 50 – 10 mattress.

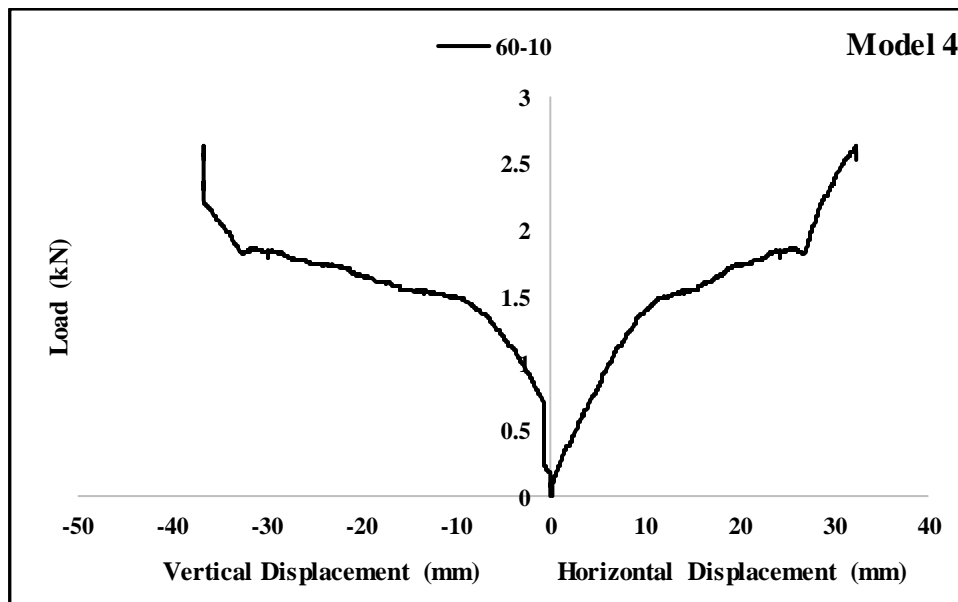


**Figure 10:** Load vs displacement curves for 60 – 10 reinforcement mattress.

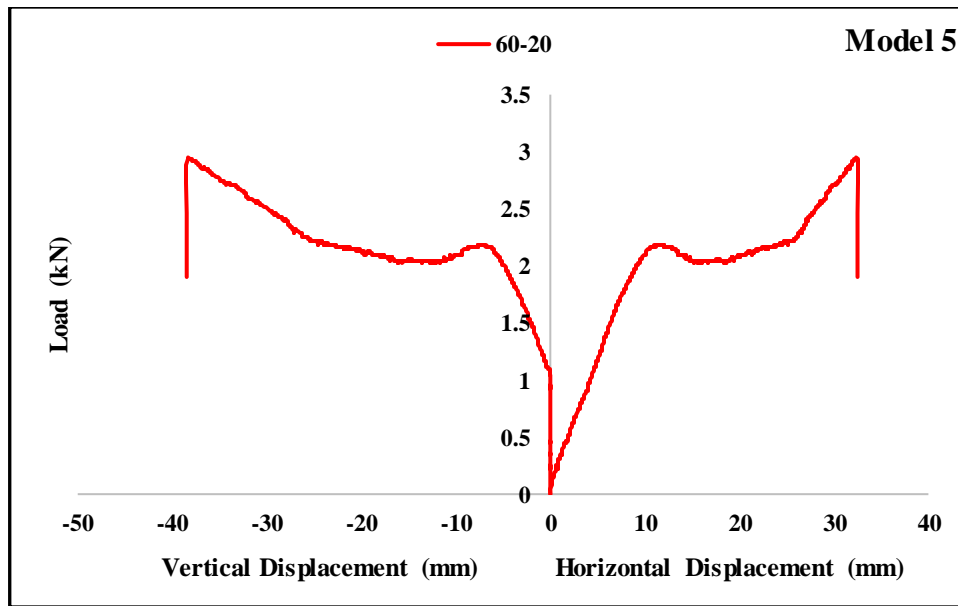


**Figure 11:** Load vs displacement curves for 60 – 20 reinforcement mattress.

The horizontal deflection and vertical settlement that occurred at maximum load in Model 3 was less than Model 2 by 9.19 mm and 5.07 mm. In Model 4 an increase in cell diameter of reinforcement mattress has increased the load carrying capacity. The maximum load resisted was 2.63 kN for which the vertical and horizontal displacements were 32.31 mm and 36.68 mm respectively. In Model 5, a 60 – 20 cellular reinforcement mattress was used which sustained a load of 2.95 kN. At this load the horizontal and vertical displacements were 32.4 mm and 38.34 mm respectively.

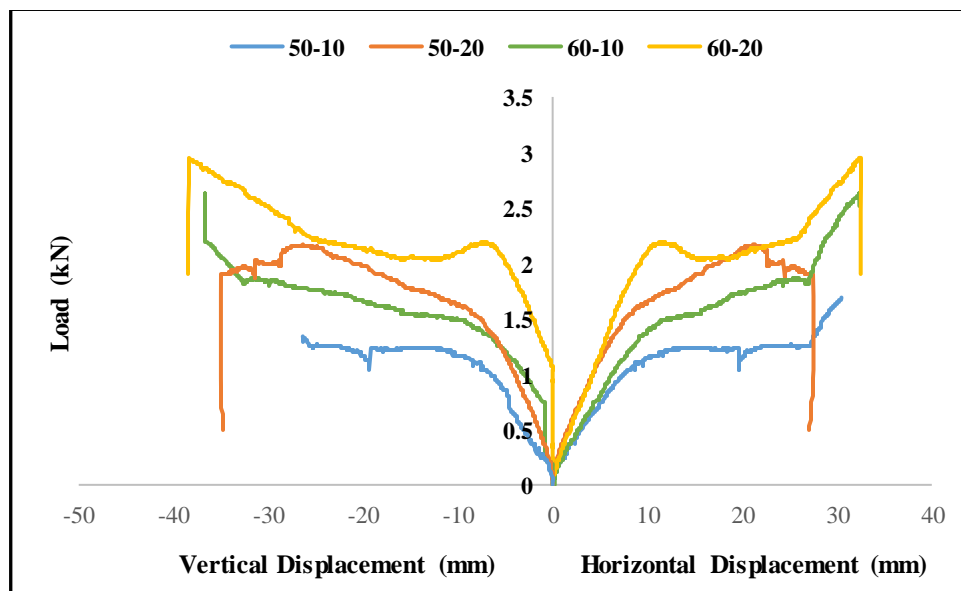


**Figure 12:** Load vs displacement curves for all Models.

Considering 1.69 kN load which was the maximum load sustained by Model 2, at this load the horizontal and vertical displacement in the remaining model are on the lower side which can

be observed from Figure 13. This signifies that an increase in diameter and height of cellular reinforcement can reduce the displacement. For the same load of 1.69 kN, the respective reduction in lateral deflection of reinforced wall for Model 3, Model 4 and Model 5 were observed as 64.4%, 39.3% and 76.2% while the corresponding vertical settlements were lowered by 62.0%, 33.5% and 90.6%.

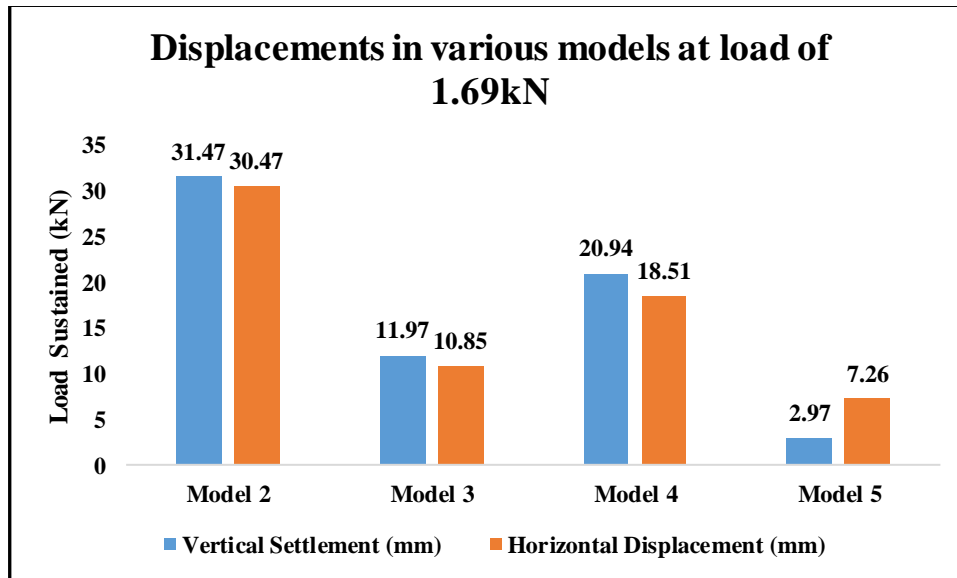


**Figure 12:** Displacements in various models at 1.69kN load

At a displacement of 10 mm in the vertical and horizontal directions for all Models excluding Model 1 the load carrying capacities were calculated. The values of load for various models at 10 mm displacement in vertical and horizontal directions are shown in Table 4. The table shows that the greatest increase in load carrying capacity in vertical and horizontal direction occurred for Model 5. When a comparison is made between these tested Models, it shows that an increase in height of cellular reinforcement has a better effect on load carrying capacity than increasing the diameter. But overall, the increase in diameter and height of cellular reinforcement have increased the performance of reinforced wall.

**Table 4:** Load carrying capacity at 10 mm displacement for various Models.

Models	At 10 mm vertical settlement (kN)		At 10 mm horizontal deflection (kN)	
	Load	% increase	Load	% increase
<b>Model 2</b>	1.17	0	1.14	0
<b>Model 3</b>	1.63	39.3	1.63	44.74
<b>Model 4</b>	1.49	27.4	1.49	21.05
<b>Model 5</b>	2.10	79.5	2.10	84.21

#### 4.0 Conclusions

The essential characterization of materials and testing of various reinforced wall Models leads to the following conclusions.

#### 4.1 Material Characterization

1. The X-Ray Fluorescence test on GBFS shows calcium oxide (CaO), Silica (SiO<sub>2</sub>), alumina (Al<sub>2</sub>O<sub>3</sub>), and magnesium oxide (MgO) as major oxides.
2. The amorphous hump between 20° to 40° shows the amorphous nature of GBFS but also presents crystalline peaks of silica which classifies GBFS as semicrystalline material.
3. It can be elucidated from the scanning electron microscopic images that GBFS is a solid and irregular shaped material.
4. Particle size distribution analysis shows that 98% of GBFS comes under the range of natural river sand.
5. Direct shear test on GBFS yields a cohesion (C) value of 8.5 N/mm<sup>2</sup> and angle of internal friction as 41°.
6. The permeability results obtained for GBFS shows it as a highly permeable material.

#### 4.2 Model testing

1. Introducing cellular reinforcement in the backfill improves the performance of retaining wall structure.
2. The increase in diameter and height of cellular reinforcement enhances the performance of reinforced wall structure.
3. Considering all the models, reinforced wall with 60 – 20 cellular reinforcement had the best performance.
4. Increasing the height of cellular reinforcement is more effective than increasing the diameter, considering the performance of reinforced wall structure.
5. At 1.69 kN load, the reduction of vertical settlement and lateral deflection for reinforced wall was 90.6% and 76.2% respectively.
6. At 10 mm vertical settlement and horizontal deflection the percentage increase in load carrying capacity was 79.5% and 84.21% respectively.

#### References

- [1] G. Q. Yang, P. Lv, B. J. Zhang, and Q. Y. Zhou, “Study on the Geogrid Reinforced Soil Retaining Wall of Concrete Rigid Face by Field Test,” *Geosynthetics in Civil and*

- Environmental Engineering. Geosynthetics Asia 2008 Proceedings of the 4th Asian Regional Conference on Geosynthetics in Shanghai*, pp. 255–260, 2008.
- [2] P. P. Capilleri, F. Ferraiolo, E. Motta, M. Scotto, and M. Todaro, “Static and dynamic analysis of two mechanically stabilized earth walls,” *Geosynth Int*, vol. 26, no. 1, pp. 26–41, Feb. 2019, doi: 10.1680/jgein.18.00034.
- [3] A. Abdelouhab, D. Dias, and N. Freitag, “Numerical analysis of the behaviour of mechanically stabilized earth walls reinforced with different types of strips,” *Geotextiles and Geomembranes*, vol. 29, no. 2, pp. 116–129, Apr. 2011, doi: 10.1016/j.geotexmem.2010.10.011.
- [4] A. W. Mekonnen and J. N. Mandal, “Model Studies on Bamboo-Geogrid Reinforced Fly Ash Walls under Uniformly Distributed Load,” *J Hazard Toxic Radioact Waste*, vol. 22, no. 2, Apr. 2018, doi: 10.1061/(asce)hz.2153-5515.0000386.
- [5] R. M. Koerner and G. R. Koerner, “A data base, statistics and recommendations regarding 171 failed geosynthetic reinforced mechanically stabilized earth (MSE) walls,” *Geotextiles and Geomembranes*, vol. 40, pp. 20–27, 2013, doi: 10.1016/j.geotexmem.2013.06.001.
- [6] Ö. Bilgin and E. Mansour, “Effect of reinforcement type on the design reinforcement length of mechanically stabilized earth walls,” *Eng Struct*, vol. 59, pp. 663–673, Feb. 2014, doi: 10.1016/j.engstruct.2013.11.013.
- [7] B. Ram, R. Lal, A. H. Padade, and J. N. Mandal, “Numerical Simulation of EPS Geofoam as Compressible Inclusions in Fly Ash Backfill Retaining Walls,” *Ground Improvement and Geosynthetics*, pp. 526–535, 2014.
- [8] A. Pant, M. Datta, and G. V. Ramana, “Bottom ash as a backfill material in reinforced soil structures,” *Geotextiles and Geomembranes*, vol. 47, no. 4, pp. 514–521, Aug. 2019, doi: 10.1016/j.geotexmem.2019.01.018.
- [9] B. K. Karnamprabhakara, U. Balunaini, A. Arulrajah, and R. Evans, “Axial Pullout Resistance and Interface Direct Shear Properties of Geogrids in Pond Ash,” *International Journal of Geosynthetics and Ground Engineering*, vol. 7, no. 2, Jun. 2021, doi: 10.1007/s40891-021-00266-x.

- [10] P. S. Prasad and G. V. Ramana, "Feasibility study of copper slag as a structural fill in reinforced soil structures," *Geotextiles and Geomembranes*, vol. 44, no. 4, pp. 623–640, Aug. 2016, doi: 10.1016/j.geotexmem.2016.03.007.
- [11] P. S. Prasad and G. V. Ramana, "Imperial smelting furnace (zinc) slag as a structural fill in reinforced soil structures," *Geotextiles and Geomembranes*, vol. 44, no. 3, pp. 406–428, Jun. 2016, doi: 10.1016/j.geotexmem.2016.01.009.
- [12] A. Kumar and A. Parihar, "Experimental study on waste foundry sand as partial replacement of retaining wall backfill," *Constr Build Mater*, vol. 402, p. 132947, Oct. 2023, doi: 10.1016/j.conbuildmat.2023.132947.
- [13] M. J. Moghadam, A. Zad, N. Mehrannia, and N. Dastaran, "Experimental evaluation of mechanically stabilized earth walls with recycled crumb rubbers," *Journal of Rock Mechanics and Geotechnical Engineering*, vol. 10, no. 5, pp. 947–957, Oct. 2018, doi: 10.1016/j.jrmge.2018.04.012.
- [14] C. S. Vieira, P. M. Pereira, and M. D. L. Lopes, "Recycled Construction and Demolition Wastes as filling material for geosynthetic reinforced structures. Interface properties," *J Clean Prod*, vol. 124, pp. 299–311, Jun. 2016, doi: 10.1016/j.jclepro.2016.02.115.
- [15] M. N. Venkatachalam and S. Balu, "A review on the application of industrial waste as reinforced earth fills in mechanically stabilized earth retaining walls," *Environmental Science and Pollution Research*, vol. 29, no. 57. Springer Science and Business Media Deutschland GmbH, pp. 86277–86297, Dec. 01, 2022. doi: 10.1007/s11356-021-17953-x.
- [16] E. Özbay, M. Erdemir, and H. I. Durmuş, "Utilization and efficiency of ground granulated blast furnace slag on concrete properties - A review," *Construction and Building Materials*, vol. 105. Elsevier Ltd, pp. 423–434, Feb. 15, 2016. doi: 10.1016/j.conbuildmat.2015.12.153.
- [17] J. Ahmad *et al.*, "A Comprehensive Review on the Ground Granulated Blast Furnace Slag (GGBS) in Concrete Production," *Sustainability (Switzerland)*, vol. 14, no. 14, Jul. 2022, doi: 10.3390/su14148783.



- [18] Z. Shao and F. Wang, “Mechanical Characteristics of Bamboo Structure and Its Components,” in *The Fracture Mechanics of Plant Materials*, Springer Singapore, 2018, pp. 125–146. doi: 10.1007/978-981-10-9017-2\_7.
- [19] Z. Ju *et al.*, “Eco-friendly method to improve the durability of different bamboo (*Phyllostachys pubescens*, Moso) sections by silver electrochemical treatment,” *Ind Crops Prod*, vol. 172, Nov. 2021, doi: 10.1016/j.indcrop.2021.113994.